HHS Public Access

Author manuscript

Mutat Res. Author manuscript; available in PMC 2015 December 30.

Published in final edited form as:

Mutat Res. 2012 June 14; 745(0): 28–37. doi:10.1016/j.mrgentox.2011.11.017.

Single-walled carbon nanotube-induced mitotic disruption⋆

L.M. Sargent[a,*], **A.F. Hubbs**[a], **S.-H. Young**[a], **M.L. Kashon**[a], **C.Z. Dinu**[b], **J.L. Salisbury**[d], **S.A. Benkovic**[e], **D.T. Lowry**[a], **A.R. Murray**[a,c], **E.R. Kisin**[a], **K.J. Siegrist**[a], **L. Battelli**[a], **J. Mastovich**[f], **J.L. Sturgeon**[f], **K.L. Bunker**[f], **A.A. Shvedova**[a,c], and **S.H. Reynolds**[a]

[a] National Institute for Occupational Safety and Health, Morgantown, WV 26505, United States

[b] College of Engineering and Mineral Resources, West Virginia University, Morgantown, WV 26506, United States

[c] Department Physiology and Pharmacology, West Virginia University, Morgantown, WV 26505, United States

[d] Department of Biochemistry, 2001st Street NW, Mayo Clinic, Rochester, MN 55905, United States

[e] NeuroScience Associates, 10915 Lake Ridge Drive, Knoxville, TN 37934, United States

[f] RJ Lee Group, Inc., 300 Hockenberg Drive, Monroeville, PA 15146, United States

Abstract

Carbon nanotubes were among the earliest products of nanotechnology and have many potential applications in medicine, electronics, and manufacturing. The low density, small size, and biological persistence of carbon nanotubes create challenges for exposure control and monitoring and make respiratory exposures to workers likely. We have previously shown mitotic spindle aberrations in cultured primary and immortalized human airway epithelial cells exposed to 24, 48 and 96 μg/cm^2 single-walled carbon nanotubes (SWCNT). To investigate mitotic spindle aberrations at concentrations anticipated in exposed workers, primary and immortalized human airway epithelial cells were exposed to SWCNT for 24–72 h at doses equivalent to 20 weeks of exposure at the Permissible Exposure Limit for particulates not otherwise regulated. We have now demonstrated fragmented centrosomes, disrupted mitotic spindles and aneuploid chromosome number at those doses. The data further demonstrated multipolar mitotic spindles comprised 95% of the disrupted mitoses. The increased multipolar mitotic spindles were associated with an increased number of cells in the G2 phase of mitosis, indicating a mitotic checkpoint response. Nanotubes were observed in association with mitotic spindle microtubules, the centrosomes and condensed chromatin in cells exposed to 0.024, 0.24, 2.4 and 24 μg/cm^2 SWCNT. Three-

⋆The findings and conclusions in this report are those of the authors and do not necessarily represent the views of the National Institute for Occupational Safety and Health.

* Corresponding author at: Toxicology and Molecular Biology Branch, Health Effects Laboratory Division, National Institute for Occupational Safety and Health, 1095 Willowdale Road, Mailstop L-3014, Morgantown, WV 26505, United States. Tel.: +1 304 285 6134; fax: +1 304 285 5708. lqs1@cdc.gov (L.M. Sargent)..

Conflict of interest statement

The authors declare that there are no conflicts of interest.

Appendix A. Supplementary data

Supplementary data associated with this article can be found, in the online version, at doi:10.1016/j.mrgentox.2011.11.017.

dimensional reconstructions showed carbon nanotubes within the centrosome structure. The lower doses did not cause cytotoxicity or reduction in colony formation after 24 h; however, after three days, significant cytotoxicity was observed in the SWCNT-exposed cells. Colony formation assays showed an increased proliferation seven days after exposure. Our results show significant disruption of the mitotic spindle by SWCNT at occupationally relevant doses. The increased proliferation that was observed in carbon nanotube-exposed cells indicates a greater potential to pass the genetic damage to daughter cells. Disruption of the centrosome is common in many solid tumors including lung cancer. The resulting aneuploidy is an early event in the progression of many cancers, suggesting that it may play a role in both tumorigenesis and tumor progression. These results suggest caution should be used in the handling and processing of carbon nanotubes.

Keywords

Aneuploid; Mitotic spindle; Genotoxicity; Nanoparticles; Nanotoxicology

1. Introduction

Carbon nanotubes are currently used in many consumer and industrial products. Current uses include electronic and drug delivery products, protective clothing, sports equipment, and space exploration. The multi-billion dollar nanotechnology industry is expected to reach a trillion dollars by 2015 [1]. Carbon nanotubes are available commercially in two major forms: single-walled carbon nanotubes (SWCNT); and the more rigid, multi-walled carbon nanotubes (MWCNT). The low density and small size of carbon nanotubes makes respiratory exposures likely, with the highest exposures expected to occur occupationally, either during production or through incorporation into various products. Although the industry is expanding rapidly, the associated human health hazards have not been investigated fully.

The durability, narrow width and proportionally greater length of the carbon nanotube are characteristics shared with asbestos and are a reason for concern [2]. While some carbon nanotubes can be degraded by myeloperoxidase in neutrophils under specific conditions [3], they may stay in the body for long periods of time following exposure. Previous investigations have demonstrated that both SWCNT and MWCNT can enter cells [4–7], and cause a variety of inflammatory, cytotoxic, proliferative and genetic changes *in vitro* and *in vivo* through a variety of mechanisms [8,9]. Nanotube exposure induced the generation of reactive oxygen species, oxidative stress and cytotoxicity [9–12]. SWCNT interacted with the structural elements of the cell, with apparent binding to the cytoskeleton [13–15], telomeric DNA [16], and G–C rich DNA sequences in the chromosomes [17]. The intercalation of SWCNT with the DNA causes a conformational change [17]. Destabilization of the DNA structure can induce chromosome breakage. *In vitro* investigations have shown SWCNT-induced DNA damage in established cancer cell lines, immortalized bronchial epithelial cells as well as primary mouse embryo fibroblasts and human mesothelial cells [18–20]. Micronuclei have been observed in significant numbers following *in vitro* treatment with SWCNT or MWCNT indicating disruption of the mitotic

spindle apparatus [19,21]. The presence of chromosome centromeres in the micronuclei indicates the loss of whole chromosomes.

In vivo studies have shown that SWCNT exposure results in macrophages without nuclei as well as dividing macrophage daughter cells connected by nanotubes, indicating SWCNT are capable of inducing errors in cell division *in vivo* [8,22]. Exposure of rodents to the larger diameter MWCNT (11.3 nm) results in micronuclei in Type II epithelial cells indicating either a high level of chromosomal breakage or mitotic spindle disruption [2]. The integrity of the mitotic spindle and chromosome number are critical because mitotic spindle disruption, centrosome damage and aneuploidy may lead to a greater risk of cancer [23–25].

Worker exposure in laboratories is likely during mixing and processing [26,27]. In commercial processing there is a potential for even higher exposures during production and processing if proper engineering controls are not used [28]. Although workplace exposures are difficult to measure, direct reading instrumentation, and filter-based methods have been used to evaluate nanoparticle concentrations and emissions to the outdoor environment of unbound engineered nanoparticles [29]. Accurate exposure assessment will be critical in evaluating the risk of nanotube exposures in workers.

The current exposure limit for carbon nanotubes falls in the class of ‘particles not otherwise regulated’ and is 5 mg/m^3 [30]. Recently, much lower exposure limits have been proposed for carbon nanotubes but are not yet recommended [31]. We, therefore, examined whether exposure to SWCNT has the potential to induce aneuploidy, mitotic spindle aberrations or disruption of the cell cycle in normal and immortalized human respiratory epithelial cells at levels that are possible in the workplace under current regulations for particulates not otherwise regulated.

2. Methods

2.1. Particles for all experiments

SWCNT (CNI Inc., Houston, TX) used in this study were produced by the high pressure CO disproportionation process (HiPco), employing CO in a continuous-flow gas phase as the carbon feedstock and $Fe(CO)_5$ as the iron-containing catalyst precursor, and were purified by acid treatment to remove metal contaminates [32]. Chemical analysis of total elemental carbon and trace metal (iron) in SWCNT was performed at the Chemical Exposure and Monitoring Branch (DART/NIOSH, Cincinnati, OH). Elemental carbon in SWCNT (HiPco) was assessed according to the NIOSH Manual of Analytical Methods [33], while metal content (iron) was determined using nitric acid dissolution and inductively coupled plasma-atomic emission spectrometry (ICP-AES, NMAM #7300). The purity of HiPco SWCNT was assessed by several standard analytical techniques including thermo-gravimetric analysis with differential scanning calorimetry, Raman spectroscopy and near-infrared (NIR) spectroscopy [34]. The specific surface area was measured at −196°C by the nitrogen absorption–desorption technique (Brunauer Emmet Teller method, BET) using a SA3100 Surface Area and Pore Size Analyzer (Beckman Coulter Inc., Fullerton, CA), while diameter and length were measured by transmission electron microscopy (TEM). The diameter and length of the purified SWCNT were 1–4 nm and 0.5–1 μm respectively. The surface area of

purified SWCNT was 1040 m^2/g. The chemical analysis was assessed at DATA CHEM Laboratories Inc. using plasma-atomic emission spectrometry where the SWCNT were defined as 99% elemental carbon and 0.23% iron. A more detailed analysis of the chemical composition has been reported previously [35]. The same lot of SWCNT was utilized for all experiments reported.

2.2. Culture of cells

Both immortalized and primary human respiratory epithelial cell populations were used to examine the potential genetic damage due to SWCNT exposure. Primary human respiratory epithelial cells (SAEC; Lonza, Walkersville, MD) isolated from the small airway of a normal human donor were examined to determine the response of a normal cell population to SWCNT exposure. The primary SAEC cells exhibited a cobblestone epithelial morphology that was free of fibroblasts during the culture period. Cells of a single lot were cultured and used between passages 1 and 6. In addition, the primary cells were examined by electron microscope and cytokeratin 8 and 18 staining to confirm the Type II phenotype. The primary cells have a normal diploid karyotype, which was necessary for the determination of potential aneuploidy induction following exposure. The primary cell cultures double every 20–24 h, which makes it possible to analyze a potential change in chromosome number and centrosome morphology of cells that have divided during a 24–72 h exposure. The mitotic index is the number of cells in mitosis when the cells are fixed. Although cells have gone through mitosis during the period of exposure, the analysis of the mitotic spindle must be performed on cells that are in division at the time of fixation. The mitotic index of the SAEC cells was 0.5% which prevented analysis of mitotic spindle integrity in this cell population.

Normal human bronchial epithelial cells (BEAS-2B) from a human donor (ATCC, Manassas, VA 20108) were immortalized with an adenovirus 12-SV40 (Ad 12SV40) as described previously [36]. BEAS-2B cells were cultured in DMEM media supplemented with 10% fetal bovine serum (Thermo Scientific, Rockford, IL), while SAEC were obtained and cultured following manufacturer's directions using Cabrex media (Lonza, Walkersville, MD). Immortalized human bronchial epithelial cell (BEAS-2B) cultures in the serum-enriched media double every 18–20 h and have normal mitotic spindle morphology (ATCC, Manassas, VA). The mitotic index of the BEAS-2B cells was 9.0 + 4.0%. The proliferation rate, the high mitotic index and the integrity of the mitotic spindle of BEAS-2B cells make it possible to examine a minimum of 100 mitotic spindles of good morphology for each of three replicate cultures for each treatment combination.

2.3. Treatment protocol

Immortalized BEAS-2B and the primary SAEC were exposed in parallel culture dishes to single-walled carbon nanotubes (SWCNT) or to the spindle poison (positive control), vanadium pentoxide (Sigma, St. Louis, MO). Vanadium pentoxide fragments the centrosome and also inhibits the assembly of microtubules resulting in aberrant spindles, aneuploidy, polyploid and binucleate cells [37]. The dose of SWCNT was based on *in vivo* exposures that demonstrated epithelial cell proliferation and abnormal nuclei at 20 μg/mouse, and is equivalent to an exposure predicted in workers of 40 h per week for 20 weeks

at the OSHA particle exposure limit (PEL) of 5 mg/m^3 for particles less than 5 μm in diameter [8,30]. The 20 μg/mouse *in vivo* dose was adjusted to the alveolar surface area of a mouse of 500 cm^2/mouse lung [38]. The adjusted dose for *in vitro* exposure was 0.02–0.08 μg/cm^2 of culture surface area. SWCNT were suspended in media and sonicated over ice for 5 min. The dispersion of the carbon nanotubes in culture media was evaluated by TEM. Vanadium pentoxide was suspended in media and sonicated over ice in the cold room for 30 min. Specifically, cultured cells were exposed to 0.024, 0.24, 2.4 or 24 μg/cm^2 SWCNT or to 0.031, 0.31 or 3.1 μg/cm^2 vanadium pentoxide. Twenty-four and 72 h after exposure, SAEC and BEAS-2B cells were prepared for analysis of apoptosis and necrosis. The SAEC cells were analyzed for centrosome integrity and chromosome number. The BEAS-2B cells were prepared for analysis of the mitotic spindle. Three independent replicates were performed for each exposure of the SAEC and BEAS-2B.

2.4. Mitotic spindle and centrosome morphology analysis

BEAS-2B and SAEC were cultured in 1-mL chamber slides. Dual chambers were prepared for each treatment and cell type. Three independent replicates were prepared for each cell type and treatment. After exposure, the media was removed and the cells were washed twice for 5 min each with 2 mL of calcium and magnesium free Dulbecco phosphate buffered saline (DPBS) + 0.1% Tween 20 (Invitrogen, Carlsbad, CA). The cells were then fixed with 100% methanol. Spindle integrity was examined using dual-label immunofluorescence for tubulin and centrin to detect the mitotic spindle and the centrosomes following methods described previously [25]. Primary antibodies were rabbit anti-beta tubulin (Abcam, La Jolla, CA, USA) and mouse anti-centrin (Salisbury Laboratory). Secondary antibodies were Rhodamine Red goat anti-rabbit IgG and Alexa 488 goat anti-mouse IgG (Invitrogen, Carlsbad, CA). Small aggregates of SWCNT (carbon nanoropes) appeared as black structures in differential interference contrast (DIC) imaging due to absorbance of light [39–41]. The morphology of the mitotic spindle and centrosome, and the relationship with carbon nanoropes, was analyzed in the BEAS-2B cells using a laser scanning confocal microscope (LSM 510, Carl Zeiss MicroImaging Inc., Thornwood, NY) as previously described [25]. To determine the association of the carbon nanoropes with the microtubules of the mitotic spindle and the centrosome, serial optical slices were obtained to create a z-stack and permit three-dimensional reconstruction using LightWave software [42]. At least 50 cells per chamber and a total of 300 cells of good centrosome and 300 cells of good mitotic spindle morphology were analyzed for each treatment dose for BEAS-2B. The morphology of the centrosome was analyzed by confocal microscopy in 300 cells for each dose and treatment in the SAEC cultures. The centrosome integrity was validated by TEM as previously described [25].

2.5. Chromosome number by FISH

Due to the necessity of a normal diploid karyotype for the analysis of chromosome number, the SAEC cells were prepared for analysis of the aneuploidy. Fluorescence in situ hybridization (FISH) for human chromosomes 1 and 4 was used to determine the chromosome number (Abbott Molecular, Des Plaines, IL) according to the guidelines of the American College of Medical Genetics [43]. To yield binucleate cells to indicate any non-disjunction of chromosomes 1 and 4, cytochalasin B was considered, however; use of this

compound inhibits uptake of carbon nanotubes by endocytosis [21]. A minimum of 100 interphase cells of good FISH morphology were analyzed to determine the number of chromosome 1 and 4. The SAEC cells were photographed using a Zeiss Axiophot microscope and Genetix Cytovision software. Cells with greater than two copies of chromosome 1 or 4 were recorded as a gain for that chromosome. Cells with less than two copies of chromosome 1 or 4 were recorded as a loss of that chromosome. The total aneuploidy was the combination of the loss and gain of both chromosomes. The experiment was repeated three times for a total of three independent replications and 300 evaluated cells per treatment and dose.

2.6. Viability and apoptosis

Triplicate cultures of BEAS-2B and SAEC cells were prepared in 96 well plates for analysis of viability using the Alamar Blue bioassay (Invitrogen, Carlsbad, CA), following procedures described previously [44]. Parallel cultures were also prepared in duplicate in 1 mL chamber slides for the analysis of apoptosis using the TUNEL assay following the manufacturer's directions (Roche, Inc., Indianapolis, IN) with some modifications outlined previously [45]. An additional positive control slide was treated with 400 Kunitz units DNase 1 (D4263, Sigma–Aldrich, St. Louis, MO). The DNase 1 fragments the DNA to simulate the fragmentation of the chromatin that occurs during apoptosis. The exposed 3-0H DNA ends were labeled with fluorescein-12-dUTP. Twenty-four hours after dosing, the cells were fixed in 4% paraformaldehyde in PBS, pH 7.4, stained with DAPI (Vector Labs, Burlingame, CA) and fluorescein (Roche), and photographed using a Zeiss Axiophot fluorescent microscope. A minimum of 50 cells were analyzed for each culture chamber for a total of one hundred cells, which was repeated three times for a total of 300 cells for each treatment and dose.

2.7. Colony formation

Triplicate cultures of BEAS-2B cells were grown in T25 flasks. When the cells were 70% confluent they were treated with SWCNT. After 24 h, the cells were trypsinized, counted and plated at 500 cells/well in 6-well plates for analysis of colony formation. After seven days, the cells were washed with PBS, stained with 10% crystal violet solution in neutral buffered formalin (Sigma, St. Louis, MO) and colonies counted.

2.8. Cell cycle analysis for DNA content

BEAS-2B cells were grown in six parallel T25 flasks. Twenty-four hours after exposure to carbon nanotubes, the cells were washed twice with PBS and removed from the dishes with 0.25% trypsin. The activity of the trypsin was stopped with DMEM media with 10% serum. The cells were then centrifuged at 300 × g at room temperature and washed with PBS. The supernatant was removed and 1×10^6 cells/mL were fixed in 70% ice-cold ethanol overnight. The fixed cells were then resuspended in 0.2 mg/mL DNase-free RNase (Sigma, St. Louis, MO) solution and incubated at 37°C for 30 min. After centrifugation at 300 × g at 4°C for 5 min, the cells were stained with 20 μg/mL propidium iodide (Sigma, St. Louis, MO) in 0.1% Triton-X (Sigma, St. Louis, MO) in PBS buffer for 30 min at room temperature. The samples were then analyzed on a FACSCalibur flow cytometer (BD Biosciences Immunocytometry Systems, San Jose, CA). The experiments were repeated

three times for a total of 18 independent replications. Data were analyzed and plotted using FlowJo v7.2.5 software.

2.9. Statistical analysis

The mean and the standard deviation were determined by the analysis of duplicate samples in three separate experiments. Chi-square analysis was used to determine statistical significance for the scoring of the mitotic spindle abnormalities and the number of cells with abnormal chromosome number. The significance of the number of viable and apoptotic cells was analyzed by ANOVA. A level of $p < 0.01$ was considered significant. For cell cycle analysis, a *t*-test was used to compare the population of G2/M in PBS and SWCNT groups. A level of $p < 0.05$ was considered significant.

3. Results

3.1. SWCNT mitotic disruption

Two human respiratory epithelial cell populations were used to examine the potential of SWCNT to induce genetic damage. To investigate SWCNT effects on respiratory cells with a normal diploid karyotype, primary small airway epithelial cells (SAEC, Lonza, Walkersville, MD) were used to examine chromosome number. The (BEAS-2B) immortalized respiratory epithelial cells were examined for the integrity of the mitotic spindle. Treatment with SWCNT induced a dose-dependent increase in the frequency of disrupted mitotic figures (Fig. 1a). Ninety-five percent of the abnormal mitotic figures in the BEAS-2B cell line were multi-polar (Fig. 1b) with only 5% being monopolar (Fig. 1b). Indeed, the pattern of the mitotic spindle disruption was similar to the pattern observed in the vanadium pentoxide-treated cells (Fig. 1b).

3.2. Chromosome number

The chromosome number was analyzed in the primary SAEC from a normal donor. The SAEC were used to assure a normal karyotype for the accurate evaluation of treatment-associated aneuploidy. FISH analysis demonstrated a loss or gain of either chromosome 1 or 4 and revealed $1.0 \pm 1.0\%$ aneuploidy in control primary respiratory cells (Fig. 1c, Table 1). The frequency of the aneuploid cells in the controls was within the range reported in adult human cells in culture [46,47]. In contrast, the SWCNT-treated SAEC had a level of aneuploidy that was as high as the effect that was observed in the vanadium pentoxide-treated positive control cells (Fig. 1c). Fig. 1d demonstrates the typical gross aneuploidy that was observed in SWCNT-treated cells. When the chromosome changes were analyzed by a loss or a gain of either chromosome 1 or 4, a significant dose response of aneuploidy was observed following carbon nanotube exposure (Table 1). The analysis of the chromosome changes by either loss or gain of chromosome 1 or 4, demonstrated that the aneuploidy was randomly distributed between alterations of chromosome 1 or chromosome 4 (Table 1). At the lowest dose of SWCNT, just over half of the observed aneuploidy was due to a gain of either chromosomes 1 or 4. However, the aneuploidy could not be explained by polyploidy because only 8% out of the total 35% aneuploid cells had a gain of both chromosomes and 16% of the aneuploid cells were due to loss of either chromosome 1 or 4. A G2 block

resulting in a polyploid 4N population, therefore, could not explain the dramatic chromosome errors.

3.3. Interaction of carbon nanotubes with mitotic spindle apparatus

SWCNT form bundles in aqueous environments due to their highly hydrophobic surfaces. Single carbon nanotubes of 1–4 nm diameter cannot be imaged; however, small bundles of nanotubes and/or nanoropes of 10 nm diameter or greater were observed using differential interference contrast imaging of the SWCNT treated cells. Cells with multipolar mitotic spindles were observed with nanoropes in the nucleus and cytoplasm (Fig. 2a–d). Physical associations were observed between SWCNT and the DNA, as well as the microtubules of the mitotic spindle apparatus (Fig. 2a–d). The multipolar mitoses had multiple centrosome fragments (Figs. 2b, e and 3b, e). The location of the nanoropes was confirmed by three-dimensional reconstructions of the serial optical images of 0.1 μm (Fig. 4a). Nanotubes were observed in association with the microtubules, the DNA, and the centrosome fragments (Fig. 4a). Furthermore, the three-dimensional reconstruction showed carbon nanotubes within the centrosome fragments (Fig. 4b). In the current investigation, SWCNT were observed in association with the centrosomes even at the lowest exposure dose.

3.4. Viability and clonal growth

The positive control, vanadium pentoxide, reduced viability 24 h after treatment (Fig. 5a). Although the mitotic disruption of the SWCNT-exposed cells was as high as the vanadium pentoxide-exposed cells, cell viability was not significantly reduced in primary respiratory epithelial cells (SAEC) or BEAS-2B cells 24 h following treatment with the SWCNT (Fig. 5a). Seventy-two hours after exposure to 0.24, 2.4 or 24 μg/cm^2 SWCNT, the viability was significantly reduced in the primary SAEC cells (Fig. 5b). The reduction in viability was observed in both BEAS-2B and SAEC cells 72 h after exposure to 0.31 μg/cm^2 vanadium pentoxide. The reduced viability was not due to the induction of apoptotic pathways as neither SWCNT nor vanadium pentoxide resulted in detectable apoptosis (data not shown). Seven days after exposure, the high dose of SWCNT resulted in a reduced number of colonies; however, the low dose exposure resulted in an increased colony formation (Fig. 5c).

3.5. Cell cycle G2 block after SWCNT treatment

The cell cycle analysis for BEAS-2B cells treated with 24 μg/cm^2 SWCNT for 24 h is shown in Fig. 6. The SWCNT-treated cells exhibit a statistically significant higher percentage of the G2/M population than in the PBS treated control cells (Table 2), indicating a G2 block in the cell cycle. The percentage of cells in the G1 phase of the cell cycle was slightly higher (+3%) and the percent of cells in S phase was lower (−6%) in SWCNT-treated cells; however, the difference was not significant. The coefficient of variance (CV) of G1 and G2/M was higher in SWCNT-treated cells than that in PBS treated cells further indicating disruption of the cell cycle in SWCNT-treated cells. The disruption of the cell cycle observed 24 h following SWCNT exposure was comparable to the level observed with the potent carcinogenic fiber asbestos [48]. The dose of carbon nanotubes was three-fold lower than the effective dose of asbestos.

4. Discussion

Our data are the first to show significant induction of multipolar mitotic spindles, aneuploidy and G2/M block of the cell cycle as well as stimulation of clonal growth in epithelial cells following exposure to concentrations of carbon nanotubes that could be anticipated during workplace exposures. Exposure to 0.024 μg SWCNT/cm^2 resulted in chromosomal aneuploidy and mitotic spindle aberrations in 35% of the cells examined. Eighty percent of the disrupted mitotic spindles were multipolar when cells were exposed to 0.024 μg SWCNT/cm^2. The distribution of multipolar mitotic spindles and centrosome fragmentation, mitotic spindle damage and aneuploidy following SWCNT exposure was similar to the effects of the genotoxin positive control, vanadium pentoxide [37]. Furthermore, three-dimensional imaging demonstrated nanotubes inside the centrosomal structure. Fragmentation of the centrosome can be induced by a number of mechanisms including global DNA damage [49], inhibition of mitotic spindle motor movement or activity [50,51], or by inhibiting the processing of misfolded centrosome proteins [52]. Levels of SWCNT four-fold higher than used in this experiment induce DNA breakage in only 8% of the cells [40]. This level of DNA damage would not result in centrosome fragmentation and this global DNA damage is unlikely to be the cause of fragmentation.

The positive control, vanadium pentoxide, is believed to induce centrosome fragmentation, mitotic spindle disruption, and aneuploidy through the inhibition of the spindle motor dynein [37,53,54]. Although inhibition of the cellular motors has not been demonstrated with carbon nanotubes, spherical nanoparticles of 40 nanometers or less have been shown to inhibit the mitotic spindle motor kinesin which is essential for normal cell division [55]. Furthermore, carbon nanotubes form hybrids with microtubules that were transported by the cellular motors [56]. The transport of the hybrid microtubules was not as efficient as that of native microtubules, indicating a partial inhibition of the kinesin activity. The coordinated activity of the mitotic motors kinesin and dynein are essential for normal cell division [57–59]. Agents that inhibit the motor activity induce mitotic spindle disruption as well as aneuploidy [60,61]. The interaction with the mitotic spindle apparatus that was observed in the current study may be due to the incorporation of SWCNT into cellular structures similar to the incorporation that has been observed in bone [62]. Indeed, the size and physical properties of SWCNT nanoropes are strikingly similar to cellular microtubules [63], suggesting SWCNT may displace some microtubules or portions of microtubules. Displacement of the microtubules by carbon nanotubes, formation of nanotubes/microtubule hybrids, and subsequent incorporation of the hybrids into the mitotic spindle may explain the strong association of the nanotubes with the mitotic apparatus [56]. Interaction of the mitotic motors with carbon nanotubes or carbon nanotube/microtubule hybrids may result in incorporation into the mitotic spindle.In addition to interactions with microtubules and the mitotic spindle, SWCNT-induced genotoxicity involves direct association with DNA. SWCNT have an affinity for G-C rich DNA sequences in the chromosomes [17]. The intercalation of SWCNT in the DNA induced a conformational change in the DNA helix [16,17] resulting in chromosome breakage and instability. In the current study, interactions between SWCNT and DNA were visualized by three-dimensional cellular reconstruction. Nanoropes integrated with the centrosome and DNA, and bridged the mitotic spindle and the

DNA. Disruption of the centrosome and the mitotic spindle are highly associated with carcinogenesis [25] thus the affinity of SWCNT for both DNA and the components of the spindle apparatus have critical implications for errors in chromosome number and potential carcinogenicity.

Exposure of rodents to SWCNT have produced mutations in K-ras [8] indicating SWCNT may be capable of inducing DNA damage *in vivo*. The demonstration of mutations of the K-ras oncogene in SWCNT-exposed mouse lungs [8] indicates genotoxicity and the potential to initiate lung cancer. Mutations of the K-ras gene are frequently reported in chemically induced mouse lung tumors and smoking-induced human lung adenocarcinoma [64–67]. Persistent epithelial proliferation is a feature of the second phase of pulmonary carcinogenesis (promotion) [68–71]. The increased colony formation of the carbon nanotube exposed cells *in vitro* indicates that low doses induce cellular proliferation. Given that epithelial hyperplasia and cellular atypia were noted in mice exposed to SWCNT and MWCNT *in vivo* [8,72,73], the potential for carcinogenicity is particularly concerning. Intraperitoneal injection of 3 mg of MWCNT with a mean length of at least 5 μm results in mesotheliomas in 87% of p53+/− transgenic mice [74] while a similar incidence of mesotheliomas was observed in rats following an intrascrotal injection of 240 μg of the long MWCNT with a median diameter of 4.5 μm [75]. A more recent study by Kanno et al., observed significant increase of mesothelioma following intraperitoneal injection of mice with as little as 50 μg of long MWCNT [76]. By contrast, intraperitoneal injection of rats with 20 mg short MWCNT with a median diameter of less than 1 μm did not result in increased mesotheliomas [77]. Although the MWCNT exposure studies have been criticized due to the high dose and the route of exposure, the studies raise concerns about the potential of cancer due to occupational and environmental exposures to particles that may have physical properties similar to asbestos fibers. Further evidence of the similarity of carbon nanotubes to asbestos was demonstrated in two recent publications showing migration of MWCNT to the subpleural tissue and entrance into the intrapleural space in a manner similar to asbestos [78,79].

The extraordinary level of chromosomal errors following SWCNT exposure underscores the importance of the SWCNT-induced damage to the mitotic spindle, the potential for direct interaction with DNA as demonstrated in the three-dimensional reconstruction of cells, and the importance of additional studies to fully elucidate the mechanism(s) of damage. Mitotic spindle damage with a predominantly multipolar phenotype and aneuploidy have also been observed following *in vitro* treatment with 0.25 μg/mL of the potent occupational carcinogen, chrysotile asbestos [80]. The ability of asbestos fibers to induce aneuploidy *in vitro* is highly correlated with the ability to induce mesotheliomas *in vivo*; this provides data supporting the importance of aneuploidy in carcinogenesis due to particulates with high aspect ratios [81]. Chrysotile has also been observed to cause a G2/M block similar to the block observed with SWCNT [48]. The dose of chrysotile used in the *in vitro* studies was three-fold higher than the lowest dose of SWCNT that induced similar damage. Chrysotile asbestos has been observed in association with DNA and in the bridge of cytokinesis; however, association with the centrosome, centrosome damage or integration with the mitotic spindle has not been documented following asbestos exposure. SWCNT-treated cells

did not die through apoptosis and had a low level of necrosis after 24–72 h of exposure. The increased colony formation one week after exposure could even suggest a hyperplastic response with resulting enhanced risk for passing genetic damage to daughter cells [68,70]. Persistent epithelial hyperplasia is characteristic of the second phase of carcinogenesis. When cell proliferation occurs prior to repair of damaged DNA, the genetic damage is passed on to subsequent generations. Given the observation that carbon nanotubes induce epithelial hyperplasia and cellular atypia in cancer resistant mice, the potential for carcinogenicity is particularly concerning [72,73,82].

While it is difficult to measure nanoparticulate concentrations in the workplace [83], our results suggest that levels of SWCNT that are possible with current regulations may exert genotoxic effects and have specific interactions with cellular components which alter the orderly progression of cell division. Similarities of the carbon nanotube to microtubules noted by Pampaloni et al., 2008 may explain the interaction with the centrosome and mitotic spindles rather than the physical interference of the spindle that occurs with fibers such as asbestos [80]. The affinity for the DNA as well as the similarity of the carbon nanotube size and physical properties to the cellular microtubules [39,63] may enhance the potential for aneuploidy. By contrast, asbestos fibers have a low affinity for the DNA but the larger asbestos fibers can physically interfere with the mitotic spindle [80]. The incorporation of the nanotubes into the centrosomal structure as well as the integration of the carbon nanotubes with the microtubules in the mitotic spindle may exert physical forces that fragment the centrosome, disrupt the mitotic spindle, and induce errors in chromosome number that are possible at the current levels of exposure. Centrosome fragmentation, mitotic spindle disruption, and aneuploidy are characteristics of cancer cells and may lead to an increased risk of cancer [23,25]. Consistent with this hypothesis, research with inorganic fibers indicate that *in vivo* asbestos-induced mesothelioma is correlated with the ability of the fiber to cause chromosomal missegregation, not with cytotoxicity [81]. The current research demonstrating mitotic spindle disruption and errors in chromosome number indicates caution should be used during the production and processing of carbon nanotubes.

Supplementary Material

Refer to Web version on PubMed Central for supplementary material.

Acknowledgments

The authors would like to thank Kimberly Clough-Thomas, NIOSH Morgantown, WV for her help with the figures. The authors would like to thank Mike Gipple, Morgantown, WV for his help with the images. The authors would like to thank Dr. John Wiley, East Carolina University for his conversations during the preparation of the manuscript.

Funding

The work was supported by NIOSH Grants: OH008282, NORA 927000Y, NORA 9927Z8V and the 7th Framework Program of the European Commission (EC-FP-7-NANOMMUNE-214281).

References

[1]. Bradley, J.; Nordan, MM.; Tassinari, O. The Recession’s Ripple Effect on Nanotech. Lux Research, Inc.; Boston, MA: 2009.

[2]. Muller J, Decordier I, Hoet PH, Lombaert N, Thomassen L, Huaux F, Lison D, Kirsch-Volders M. Clastogenic and aneugenic effects of multi-wall carbon nanotubes in epithelial cells. Carcinogenesis. 2008; 29:427–433. [PubMed: 18174261]

[3]. Kagan VE, Konduru NV, Feng W, Allen BL, Conroy J, Volkov Y, Vlasova II, Belikova NA, Yanamala N, Kapralov A, Tyurina YY, Shi J, Kisin ER, Murray AR, Franks J, Stolz D, Gou P, Klein-Seetharaman J, Fadeel B, Star A, Shvedova AA. Carbon nanotubes degraded by neutrophil myeloperoxidase induce less pulmonary inflammation. Nat. Nanotechnol. 2010; 5:354–359. [PubMed: 20364135]

[4]. Bottini M, Balasubramanian C, Dawson MI, Bergamaschi A, Bellucci S, Mustelin T. Isolation and characterization of fluorescent nanoparticles from pristine and oxidized electric arc-produced single-walled carbon nanotubes. J. Phys. Chem. B: Condens. Matter Mater. Surf. Interfaces Biophys. 2006; 110:831–836. [PubMed: 16471611]

[5]. Bottini M, Bruckner S, Nika K, Bottini N, Bellucci S, Magrini A, Bergamaschi A, Mustelin T. Multi-walled carbon nanotubes induce T lymphocyte apoptosis. Toxicol. Lett. 2006; 160:121–126. [PubMed: 16125885]

[6]. Monteiro-Riviere NA, Nemanich RJ, Inman AO, Wang YY, Riviere JE. Multi-walled carbon nanotube interactions with human epidermal keratinocytes. Toxicol. Lett. 2005; 155:377–384. [PubMed: 15649621]

[7]. Worle-Knirsch JM, Pulskamp K, Krug HF. Oops they did it again! Carbon nanotubes hoax scientists in viability assays. Nano Lett. 2006; 6:1261–1268. [PubMed: 16771591]

[8]. Shvedova AA, Kisin E, Murray AR, Johnson VJ, Gorelik O, Arepalli S, Hubbs AF, Mercer RR, Keohavong P, Sussman N, Jin J, Yin J, Stone S, Chen BT, Deye G, Maynard A, Castranova V, Baron PA, Kagan VE. Inhalation vs. aspiration of single-walled carbon nanotubes in C57BL/6 mice: inflammation, fibrosis, oxidative stress, and mutagenesis. Am. J. Physiol. Lung Cell. Mol. Physiol. 2008; 295:L552–L565. [PubMed: 18658273]

[9]. Shvedova AA, Kisin ER, Mercer R, Murray AR, Johnson VJ, Potapovich AI, Tyurina YY, Gorelik O, Arepalli S, Schwegler-Berry D, Hubbs AF, Antonini J, Evans DE, Ku BK, Ramsey D, Maynard A, Kagan VE, Castranova V, Baron P. Unusual inflammatory and fibrogenic pulmonary responses to single-walled carbon nanotubes in mice. Am. J. Physiol. Lung Cell. Mol. Physiol. 2005; 289:L698–L708. [PubMed: 15951334]

[10]. Lam CW, James JT, McCluskey R, Hunter RL. Pulmonary toxicity of single-wall carbon nanotubes in mice 7 and 90 days after intratracheal instillation. Toxicol. Sci. 2004; 77:126–134. [PubMed: 14514958]

[11]. Risom L, Moller P, Loft S. Oxidative stress-induced DNA damage by particulate air pollution. Mutat. Res. 2005; 592:119–137. [PubMed: 16085126]

[12]. Warheit DB, Laurence BR, Reed KL, Roach DH, Reynolds GA, Webb TR. Comparative pulmonary toxicity assessment of single-wall carbon nanotubes in rats. Toxicol. Sci. 2004; 77:117–125. [PubMed: 14514968]

[13]. Porter AE, Gass M, Muller K, Skepper JN, Midgley PA, Welland M. Direct imaging of single-walled carbon nanotubes in cells. Nat. Nanotechnol. 2007; 2:713–717. [PubMed: 18654411]

[14]. Holt BD, Short PA, Rape AD, Wang YL, Islam MF, Dahl KN. Carbon nanotubes reorganize actin structures in cells and ex vivo. ACS Nano. 2010; 4:4872–4878. [PubMed: 20669976]

[15]. Walker VG, Li Z, Hulderman T, Schwegler-Berry D, Kashon ML, Simeonova PP. Potential *in vitro* effects of carbon nanotubes on human aortic endothelial cells. Toxicol. Appl. Pharmacol. 2009; 236:319–328. [PubMed: 19268679]

[16]. Li X, Peng Y, Ren J, Qu X. Carboxyl-modified single-walled carbon nanotubes selectively induce human telomeric i-motif formation. Proc. Natl. Acad. Sci. U.S.A. 2006; 103:19658–19663. [PubMed: 17167055]

[17]. Li X, Peng Y, Qu X. Carbon nanotubes selective destabilization of duplex and triplex DNA and inducing B–A transition in solution. Nucleic Acids Res. 2006; 34:3670–3676. [PubMed: 16885240]

[18]. Kisin ER, Murray AR, Keane MJ, Shi XC, Schwegler-Berry D, Gorelik O, Arepalli S, Castranova V, Wallace WE, Kagan VE, Shvedova AA. Single-walled carbon nanotubes: geno-

and cytotoxic effects in lung fibroblast V79 cells. J. Toxicol. Environ. Health A. 2007; 70:2071–2079. [PubMed: 18049996]

[19]. Lindberg HK, Falck GC, Suhonen S, Vippola M, Vanhala E, Catalan J, Savolainen K, Norppa H. Genotoxicity of nanomaterials: DNA damage and micronuclei induced by carbon nanotubes and graphite nanofibres in human bronchial epithelial cells *in vitro*. Toxicol. Lett. 2009; 186:166–173. [PubMed: 19114091]

[20]. Pacurari M, Yin XJ, Zhao J, Ding M, Leonard SS, Schwegler-Berry D, Ducatman BS, Sbarra D, Hoover MD, Castranova V, Vallyathan V. Raw single-wall carbon nanotubes induce oxidative stress and activate MAPKs, AP-1, NF-kappaB, and Akt in normal and malignant human mesothelial cells. Environ. Health Perspect. 2008; 116:1211–1217. [PubMed: 18795165]

[21]. Doak SH, Griffiths SM, Manshian B, Singh N, Williams PM, Brown AP, Jenkins GJ. Confounding experimental considerations in nanogenotoxicology. Mutagenesis. 2009; 24:285–293. [PubMed: 19351890]

[22]. Mangum JB, Turpin EA, Antao-Menezes A, Cesta MF, Bermudez E, Bonner JC. Single-walled carbon nanotube (SWCNT)-induced interstitial fibrosis in the lungs of rats is associated with increased levels of PDGF mRNA and the formation of unique intercellular carbon structures that bridge alveolar macrophages in situ. Part. Fibre Toxicol. 2006; 3:15. [PubMed: 17134509]

[23]. Aardema MJ, Albertini S, Arni P, Henderson LM, Kirsch-Volders M, Mackay JM, Sarrif AM, Stringer DA, Taalman RD. Aneuploidy: a report of an ECETOC task force. Mutat. Res. 1998; 410:3–79. [PubMed: 9587424]

[24]. Fukasawa K. Centrosome amplification, chromosome instability and cancer development. Cancer Lett. 2005; 230:6–19. [PubMed: 16253756]

[25]. Salisbury JL, D'Assoro AB, Lingle WL. Centrosome amplification and the origin of chromosomal instability in breast cancer. J. Mammary Gland Biol. Neoplasia. 2004; 9:275–283. [PubMed: 15557800]

[26]. Han JH, Lee EJ, Lee JH, So KP, Lee YH, Bae GN, Lee SB, Ji JH, Cho MH, Yu IJ. Monitoring multiwalled carbon nanotube exposure in carbon nanotube research facility. Inhal. Toxicol. 2008; 20:741–749. [PubMed: 18569096]

[27]. Johnson DR, Methner MM, Kennedy AJ, Steevens JA. Potential for occupational exposure to engineered carbon-based nanomaterials in environmental laboratory studies. Environ. Health Perspect. 2010; 118:49–54. [PubMed: 20056572]

[28]. Methner M, Hodson L, Geraci C. Nanoparticle emission assessment technique (NEAT) for the identification and measurement of potential inhalation exposure to engineered nanomaterials. Part A. J. Occup. Environ. Hyg. 2010; 7:127–132. [PubMed: 20017054]

[29]. Casuccio G, Ogle R, Bunker K, Rickabaugh K, Wahl L, Roberts T, Pauer R. Worker and Environmental Assessment of Potential Unbound Engineered Nanoparticle Releases. Phase III Final Report. 2010

[30]. OSHA. Limits for Air Contaminants: Occupational Safety and Health Standards. Occupational Safety and Health Administration. 2006

[31]. DHHS/CDC/NIOSH. Occupational Exposure to Carbon Nanotubes and Nanofibers, Department of Health and Human Services, Centers for Disease Control and Prevention. National Institute for Occupational Safety and Health. 2010:114–115.

[32]. Gorelik, O.; Nikolaev, P.; Arepalli, S. Purification procedures for single-walled carbon nanotubes. NASA Contractor Report; Hanover, MD: 2000.

[33]. Birch, ME. Monitoring of Diesel Exhaust Particulate in the Workplace. 4th. DHHS; Cincinnati, OH: 2003.

[34]. Arepalli S, Nikolaev P, Gorelik O, Hadjiev VG, Bradlev HA, Holmes W, Files B, Yowell L. Protocol for the characterization of single-wall carbon nanotube material quality. Carbon. 2004; 42:1783–1791.

[35]. Shvedova AA, Kisin ER, Murray AR, Sargent L, Lowry D, Chirila M, Siegrist KJ, Schwegler-Berry D, Leonard S, Castranova V, Fadeel B, Kagan VE. Genotoxicity of carbon nanofibers: are they potentially more or less dangerous than carbon nanotubes or asbestos? Toxicol. Appl. Pharmacol. 2011; 252:1–10. [PubMed: 21310169]

[36]. Lechner JF, Neft RE, Gilliland FD, Crowell RE, Auckley DH, Temes RT, Belinsky SA. Individuals at high risk for lung cancer have airway epithelial cells with chromosome aberrations frequently found in lung tumor cells. In Vivo. 1998; 12:23–26. [PubMed: 9575422]

[37]. Ramirez P, Eastmond DA, Laclette JP, Ostrosky-Wegman P. Disruption of microtubule assembly and spindle formation as a mechanism for the induction of aneuploid cells by sodium arsenite and vanadium pentoxide. Mutat. Res. 1997; 386:291–298. [PubMed: 9219566]

[38]. Stone KC, Mercer RR, Gehr P, Stockstill B, Crapo JD. Allometric relationships of cell numbers and size in the mammalian lung. Am. J. Respir. Cell Mol. Biol. 1992; 6:235–243. [PubMed: 1540387]

[39]. Mercer RR, Scabilloni J, Wang L, Kisin E, Murray AR, Schwegler-Berry D, Shvedova AA, Castranova V. Alteration of deposition pattern and pulmonary response as a result of improved dispersion of aspirated single-walled carbon nanotubes in a mouse model. Am. J. Physiol. Lung Cell. Mol. Physiol. 2008; 294:L87–L97. [PubMed: 18024722]

[40]. Sargent LM, Shvedova AA, Hubbs AF, Salisbury JL, Benkovic SA, Kashon ML, Lowry DT, Murray AR, Kisin ER, Friend S, McKinstry KT, Battelli L, Reynolds SH. Induction of aneuploidy by single-walled carbon nanotubes. Environ. Mol. Mutagen. 2009; 50:708–717. [PubMed: 19774611]

[41]. Sargent L, Shvedova AA, Hubbs AF, Lowry DT, Kashon ML, Murray A, Kisin E, Benkovic SA, Miller DB, McKinstry KT, Reynolds SH. Induction of aneuploidy by single walled carbon nanotubes. Toxicol. Sci. Suppl. 2009

[42]. Haas A, Fischer MS. Three-dimensional reconstruction of histological sections using modern product-design software. Anat. Rec. 1997; 249:510–516. [PubMed: 9415459]

[43]. ACMG. Standards and guidelines for Clinical Genetics Laboratories, in: Documentation of FISH Results. American College of Medical Genetics; Bethesda, MD: 2006.

[44]. Keane RW, Srinivasan A, Foster LM, Testa MP, Ord T, Nonner D, Wang HG, Reed JC, Bredesen DE, Kayalar C. Activation of CPP32 during apoptosis of neurons and astrocytes. J. Neurosci. Res. 1997; 48:168–180. [PubMed: 9130145]

[45]. Gavrieli Y, Sherman Y, Ben-Sasson SA. Identification of programmed cell death in situ via specific labeling of nuclear DNA fragmentation. J. Cell Biol. 1992; 119:493–501. [PubMed: 1400587]

[46]. Wiktor AE, Van Dyke DL, Stupca PJ, Ketterling RP, Thorland EC, Shearer BM, Fink SR, Stockero KJ, Majorowicz JR, Dewald GW. Preclinical validation of fluorescence in situ hybridization assays for clinical practice. Genet. Med. 2006; 8:16–23. [PubMed: 16418595]

[47]. Yurov YB, Iourov IY, Monakhov VV, Soloviev IV, Vostrikov VM, Vorsanova SG. The variation of aneuploidy frequency in the developing and adult human brain revealed by an interphase FISH study. J. Histochem. Cytochem. 2005; 53:385–390. [PubMed: 15750026]

[48]. Cortez BD, Quassollo G, Caceres A, Machado-Santelli GM. The fate of chrysotile-induced multipolar mitosis and aneuploid population in cultured lung cancer cells. PLoS One. 2011; 6

[49]. Hut HM, Lemstra W, Blaauw EH, Van Cappellen GW, Kampinga HH, Sibon OC. Centrosomes split in the presence of impaired DNA integrity during mitosis. Mol. Biol. Cell. 2003; 14:1993–2004. [PubMed: 12802070]

[50]. Abal M, Keryer G, Bornens M. Centrioles resist forces applied on centrosomes during G2/M transition. Biol. Cell. 2005; 97:425–434. [PubMed: 15898952]

[51]. Krzysiak TC, Wendt T, Sproul LR, Tittmann P, Gross H, Gilbert SP, Hoenger A. A structural model for monastrol inhibition of dimeric kinesin Eg5. EMBO J. 2006; 25:2263–2273. [PubMed: 16642039]

[52]. Ehrhardt AG, Sluder G. Spindle pole fragmentation due to proteasome inhibition. J. Cell. Physiol. 2005; 204:808–818. [PubMed: 15828030]

[53]. Evans JA, Mocz G, Gibbons IR. Activation of dynein 1 adenosine triphosphatase by monovalent salts and inhibition by vanadate. J. Biol. Chem. 1986; 261:14039–14043. [PubMed: 2945815]

[54]. Ma S, Trivinos-Lagos L, Graf R, Chisholm RL. Dynein intermediate chain mediated dynein-dynactin interaction is required for interphase microtubule organization and centrosome replication and separation in Dictyostelium. J. Cell Biol. 1999; 147:1261–1274. [PubMed: 10601339]

[55]. Bachand M, Trent AM, Bunker BC, Bachand GD. Physical factors affecting kinesin-based transport of synthetic nanoparticle cargo. J. Nanosci. Nanotechnol. 2005; 5:718–722. [PubMed: 16010927]

[56]. Dinu CZ, Bale SS, Zhu G, Dordick JS. Tubulin encapsulation of carbon nanotubes into functional hybrid assemblies. Small. 2009; 5:310–315. [PubMed: 19148890]

[57]. Heald R. Motor function in the mitotic spindle. Cell. 2000; 102:399–402. [PubMed: 10966101]

[58]. McIntosh JR, Grishchuk EL, West RR. Chromosome-microtubule interactions during mitosis. Annu. Rev. Cell Dev. Biol. 2002; 18:193–219. [PubMed: 12142285]

[59]. Zimmerman W, Doxsey SJ. Construction of centrosomes and spindle poles by molecular motor-driven assembly of protein particles. Traffic. 2000; 1:927–934. [PubMed: 11208082]

[60]. Mayer TU, Kapoor TM, Haggarty SJ, King RW, Schreiber SL, Mitchison TJ. Small molecule inhibitor of mitotic spindle bipolarity identified in a phenotype-based screen. Science. 1999; 286:971–974. [PubMed: 10542155]

[61]. Ochi T. Role of mitotic motors, dynein and kinesin, in the induction of abnormal centrosome integrity and multipolar spindles in cultured V79 cells exposed to dimethylarsinic acid. Mutat. Res. 2002; 499:73–84. [PubMed: 11804606]

[62]. Aoki N, Akasaka T, Watari F, Yokoyama A. Carbon nanotubes as scaffolds for cell culture and effect on cellular functions. Dent. Mater. J. 2007; 26:178–185. [PubMed: 17621932]

[63]. Pampaloni F, Florin EL. Microtubule architecture: inspiration for novel carbon nanotube-based biomimetic materials. Trends Biotechnol. 2008; 26:302–310. [PubMed: 18433902]

[64]. Chan PC, Peckham JC, Bristol DW, Bucher JR, Burka LT, Chhabra RS, Herbert RA, King-Herbert AP, Kissling GE, Malarkey DE, Peddada SD, Roycroft JH, Smith CS, Travlos GS, Witt KL, Sills KL. Toxicology and carcinogenesis studies of cumene in F344/N rats and B6C3F1 mice (inhalation studies). NTP TR 542 National Toxicology Program. 2007:1–104.

[65]. Hong HH, Dunnick J, Herbert R, Devereux TR, Kim Y, Sills RC. Genetic alterations in K-ras and p53 cancer genes in lung neoplasms from Swiss (CD-1) male mice exposed transplacentally to AZT. Environ. Mol. Mutagen. 2007; 48:299–306. [PubMed: 16395694]

[66]. Pao W, Miller V, Zakowski M, Doherty J, Politi K, Sarkaria I, Singh B, Heelan R, Rusch V, Fulton L, Mardis E, Kupfer D, Wilson R, Kris M, Varmus H. EGF receptor gene mutations are common in lung cancers from never smokers and are associated with sensitivity of tumors to gefitinib and erlotinib. Proc. Natl. Acad. Sci. U.S.A. 2004; 101:13306–13311. [PubMed: 15329413]

[67]. Tam IY, Chung LP, Suen WS, Wang E, Wong MC, Ho KK, Lam WK, Chiu SW, Girard L, Minna JD, Gazdar AF, Wong MP. Distinct epidermal growth factor receptor and KRAS mutation patterns in non-small cell lung cancer patients with different tobacco exposure and clinicopathologic features. Clin. Cancer Res. 2006; 12:1647–1653. [PubMed: 16533793]

[68]. Pitot HC. Stage-specific gene expression during hepatocarcinogenesis in the rat. J. Cancer Res. Clin. Oncol. 1996; 122:257–265. [PubMed: 8609148]

[69]. Pitot HC. Adventures in hepatocarcinogenesis. Annu. Rev. Pathol. 2007; 2:1–29. [PubMed: 18039091]

[70]. Pitot HC, Campbell HA, Maronpot R, Bawa N, Rizvi TA, Xu YH, Sargent L, Dragan Y, Pyron M. Critical parameters in the quantitation of the stages of initiation, promotion, and progression in one model of hepatocarcinogenesis in the rat. Toxicol. Pathol. 1989; 17:594–611. (discussion 592–611). [PubMed: 2697939]

[71]. Rubin H. Synergistic mechanisms in carcinogenesis by polycyclic aromatic hydrocarbons and by tobacco smoke: a bio-historical perspective with updates. Carcinogenesis. 2001; 22:1903–1930. [PubMed: 11751421]

[72]. Hubbs AF, Mercer RR, Coad JE, Battelli LA, Willard P, Sriram K, Wolfarth M, Castranova V, Porter D. Persistent pulmonary inflammation, airway mucous metaphasia and migration of multi-walled carbon nanotubes from the lung after subchronic exposure. The Toxicologist. 2009; 108:2193.

[73]. Porter DW, Hubbs AF, Mercer RR, Wu N, Wolfarth MG, Sriram K, Leonard S, Battelli L, Schwegler-Berry D, Friend S, Andrew M, Chen BT, Tsuruoka S, Endo M, Castranova V. Mouse

pulmonary dose- and time course-responses induced by exposure to multi-walled carbon nanotubes. Toxicology. 2010; 269:136–147. [PubMed: 19857541]

[74]. Takagi A, Hirose A, Nishimura T, Fukumori N, Ogata A, Ohashi N, Kitajima S, Kanno J. Induction of mesothelioma in p53+/− mouse by intraperitoneal application of multi-wall carbon nanotube. J. Toxicol. Sci. 2008; 33:105–116. [PubMed: 18303189]

[75]. Sakamoto Y, Nakae D, Fukumori N, Tayama K, Maekawa A, Imai K, Hirose A, Nishimura T, Ohashi N, Ogata A. Induction of mesothelioma by a single intrascrotal administration of multi-wall carbon nanotube in intact male Fischer 344 rats. J. Toxicol. Sci. 2009; 34:65–76. [PubMed: 19182436]

[76]. Kanno, J.; Takagi, A.; Nishimura, T.; Hlrose, A. The Toxicologist. Oxford University Press; Salt Lake City, UT: 2010. Mesothelioma induction by micrometer-sized multi-walled carbon nanotube intraperitoneally injected to p53 heterozygous mice; p. A1397

[77]. Muller J, Delos M, Panin N, Rabolli V, Huaux F, Lison D. Absence of carcinogenic response to multiwall carbon nanotubes in a 2-year bioassay in the peritoneal cavity of the rat. Toxicol. Sci. 2009; 110:442–448. [PubMed: 19429663]

[78]. Mercer RR, Hubbs AF, Scabilloni JF, Wang L, Battelli LA, Schwegler-Berry D, Castranova V, Porter DW. Distribution and persistence of pleural penetrations by multi-walled carbon nanotubes. Part. Fibre Toxicol. 2010; 7:28. [PubMed: 20920331]

[79]. Ryman-Rasmussen JP, Cesta MF, Brody AR, Shipley-Phillips JK, Everitt JI, Tewksbury EW, Moss OR, Wong BA, Dodd DE, Andersen ME, Bonner JC. Inhaled carbon nanotubes reach the subpleural tissue in mice. Nat. Nanotechnol. 2009; 4:747–751. [PubMed: 19893520]

[80]. Cortez BA, Machado-Santelli GM. Chrysotile effects on human lung cell carcinoma in culture: 3-D reconstruction and DNA quantification by image analysis. BMC Cancer. 2008; 8:181. [PubMed: 18588678]

[81]. Yegles M, Janson X, Dong HY, Renier A, Jaurand MC. Role of fibre characteristics on cytotoxicity and induction of anaphase/telophase aberrations in rat pleural mesothelial cells *in vitro*: correlations with *in vivo* animal findings. Carcinogenesis. 1995; 16:2751–2758. [PubMed: 7586195]

[82]. Shvedova AA, Fabisiak JP, Kisin ER, Murray AR, Roberts JR, Tyurina YY, Antonini JM, Feng WH, Kommineni C, Reynolds J, Barchowsky A, Castranova V, Kagan VE. Sequential exposure to carbon nanotubes and bacteria enhances pulmonary inflammation and infectivity. Am. J. Respir. Cell Mol. Biol. 2008; 38:579–590. [PubMed: 18096873]

[83]. Hubbs A, Castranova V, Chen BT, Frazer DG, McKinney W, Mercer RR, Kashon ML, Battelli LA, Willard P, Porter DW. Pulmonary inflammation, epithelial hyperplasia, and lymph node translocation after multi-walled carbon nanotube inhalation. The Toxicologist. 2011; 120:11. (abstract #58).

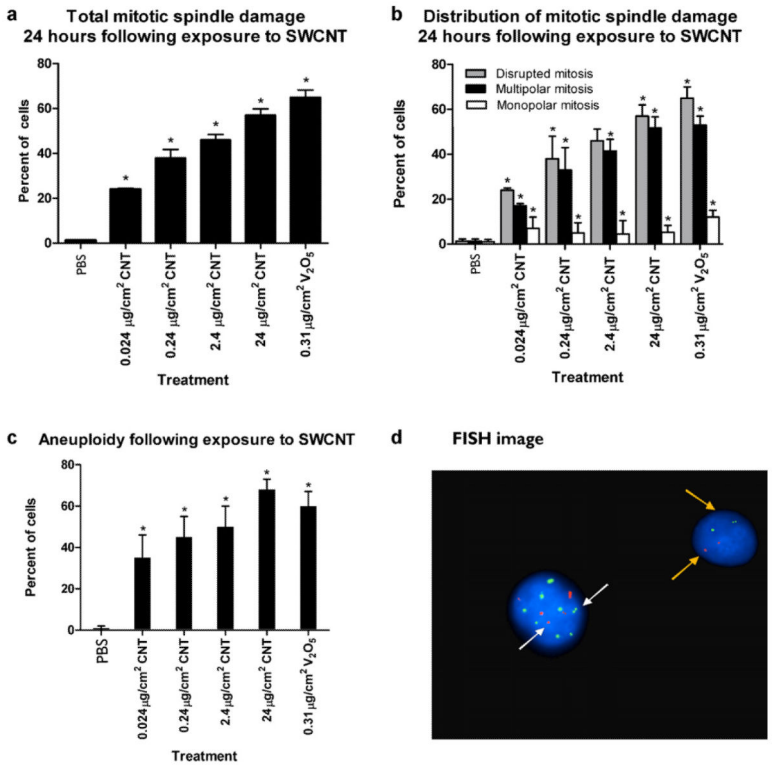

Fig. 1.

(a–d) The bar graph shows the percentage of BEAS-2B cells that were observed with mitotic spindle abnormalities. Mitotic spindle abnormalities are expressed as a percent of cells with a mitotic disruption. The solid bars indicate the percent of cells in the control and exposed SAEC cells with mitotic spindle abnormalities. The abnormalities included monopolar, tripolar and quadrapolar mitotic spindles. (b) The bar graph shows the distribution of the mitotic spindle abnormalities in BEAS-2B cells that were monopolar or multipolar compared to the total number of disrupted mitoses. The solid bars indicate the percent of total mitotic figures that had a multipolar mitotic spindle; the white bars indicate the percent of total mitotic figures that had a monopolar mitotic spindle. The gray bars indicate the percent of cells with either a monopolar or multipolar mitotic spindle. (c) The bar graph demonstrates the percent of SAEC with an aneuploid chromosome number 24 h following exposure to SWCNT or the positive control V_2O_5. The solid bars indicate the percent of cells with errors in chromosome number in the SWCNT, vanadium pentoxide and diluent control SAEC cells. *Significantly different from the unexposed control cells at $p < 0.001$. (d) A photograph of a FISH image of two cells treated with 0.24 μg/cm^2 SWCNT. The cell indicated by white arrows has 8 green signals (chromosome 4) and 5 (chromosome 1) red signals. Yellow arrows show a normal cell with two green signals and two red signals. This figure demonstrates the typical gross aneuploidy that was observed with SWCNT.

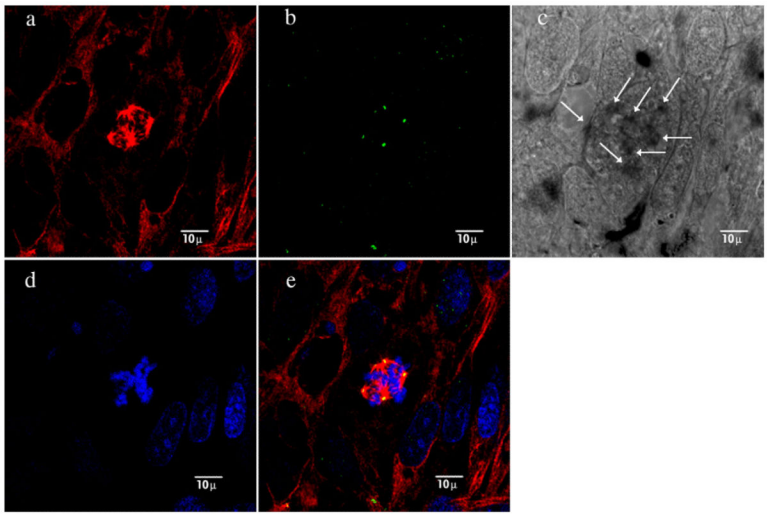

Fig. 2.

(a–d) SWCNT-treated cell with 4 spindle poles: the photographs in (a)–(e) show a multipolar mitotic spindle with four poles. The mitotic tubulin in (a) is red, the centrosomes in (b) are green, the nanotubes in (c) are black and the DNA is blue in (d). (e) The composite of tubulin, DNA and spindle poles. The nanotubes in (c) can be seen in the nucleus in association with microtubules and the DNA as indicated by white arrows. Serial optical sections at 0.1 μm intervals using confocal microscopy confirmed the location of the nanotubes. The scale bar indicates 10 μm units.

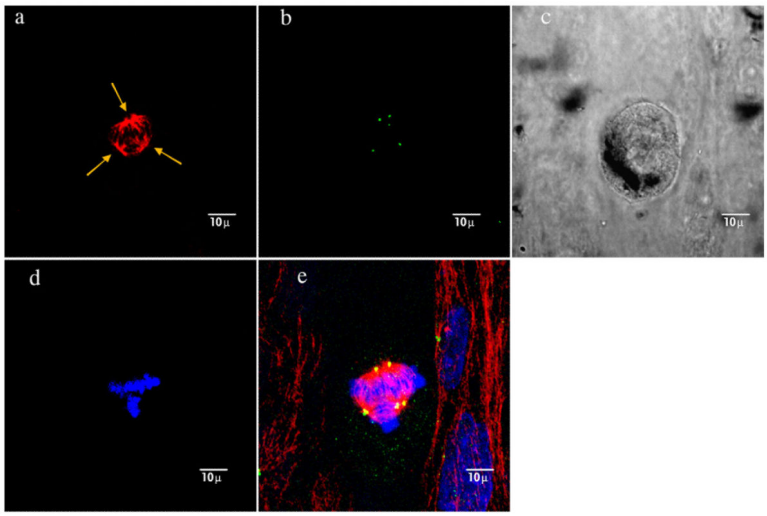

Fig. 3.

Typical tripolar mitosis viewed by confocal immunofluorescent and DIC microscopy: (a) spindle disruption by SWCNT is demonstrated using indirect immunofluorescence to stain tubulin red and reveal the microtubules. (b) Spindle poles are stained green. (c) The SWCNT are black when viewed using DIC. (d) DNA stains blue using DAPI. (e) The composite image demonstrates the three poles directing the DNA in three directions rather than two opposing poles seen in the normal bipolar mitosis. Each of the three poles is indicated by yellow arrows.

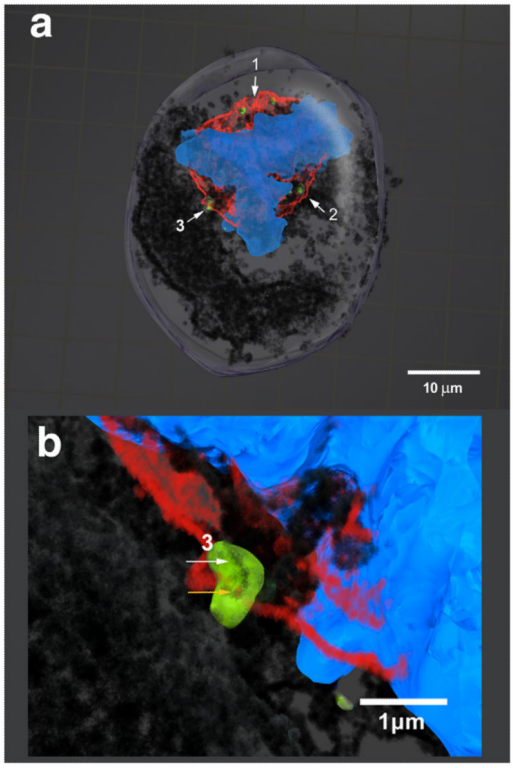

Fig. 4.

(a) A 3D reconstruction of the multipolar mitotic spindle with three poles. The DNA is blue, the tubulin is red, the centrosomes are green and the nanotubes are black in (a) and (b). The three spindle poles are indicated by white arrows. Serial optical sections of 0.1 μm in depth were used to construct a 3D image of the tripolar mitosis. The reconstructed image shows nanotubes inside the cell in association with each centrosome fragment at the 3 spindle poles. Nanotubes are also integrated with the microtubules and the DNA. In (b), the centrosomes and the portion of the mitotic spindle labeled as region 3 in (a) are increased in size to show details of the nanotube association with the centrosome and the tubulin. The nanotubes can be seen within the centrosome structure as indicated by the white arrow. The nanotubes associated with the microtubule can also be seen in more detail as indicated by the yellow arrow. In this cell, the three spindle poles, the three unequal DNA bundles, and the disruption of microtubule attachments to two centrosomes suggest major perturbations in cell division.

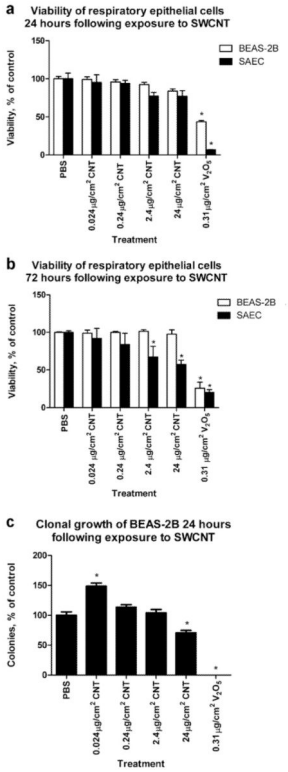

Fig. 5.

(a) The bar graph shows viability of BEAS-2B and SAEC cells at 24 h following exposure to SWCNT or V_2O_5. The black bars indicate the level of viability in control and exposed SAEC cells. The white bars indicate the degree of viability in the exposed and control BEAS-2B cells. (b) The bar graph shows viability of BEAS-2B and SAEC cells at 72 h following exposure to SWCNT or V_2O_5. The black bars indicate the level of viability in control and exposed SAEC cells. The white bars indicate the level in the exposed and control BEAS-2B cells. (c) The bar graph shows clonal growth in the BEAS-2B cells 7 days after exposure to SWCNT. The solid bars indicate the mean number of colonies; *statistical significance at $p < 0.001$.

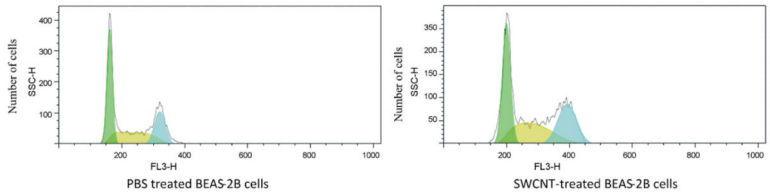

Fig. 6.

Cell cycle analysis of SWCNT-treated BEAS-2B cells. A typical flow cytometry cell cycle analysis of BEAS-2B cells treated with PBS (left panel) or 24 μg/mL SWCNT for 24 h (right panel). The percentage of G2/M population in SWCNT-treated BEAS-2B cells was statistically significantly higher than that in the PBS treated control cells, which indicated a G2 block in cell cycle.

Table 1

Percent of chromosome errors in SAEC cells following treatment with SWCNT and percent of chromosome errors in SAEC cells following treatment with V2O5.

	Total % aneuploid cells	Change in chromosome 1 (%)	Gain of chromosome 1 (%)	Change in chromosome 4 (%)	Gain of chromosome 4 (%)	Change in both chromosomes (%)
Dose SWCNT						
0	2.25 ± 1.0	1.0 ± 1.0	1.0 ± 1.0	1.25 ± 1.0	1.0 ± 1.0	0
0.024 μg/cm^2	35 ± 11*	21 ± 4*	13 ± 4*	22 ± 3*	10 ± 2*	8 ± 3*
0.24 μg/cm^2	45 ± 10*	30 ± 6*	20 ± 10*	28 ± 5*	21 ± 9*	14 ± 5*
2.4 μg/cm^2	50 ± 10*	32 ± 4*	23 ± 10*	31 ± 3*	25 ± 10*	13 ± 3*
24 μg/cm^2	68 ± 5*	37 ± 5*	23 ± 5*	35 ± 11*	25 ± 5*	19 ± 5*
Dose vanadium						
0.31 μg/cm^2	60 ± 7*	50 ± 7*	41 ± 5*	51 ± 11*	42 ± 6*	38 ± 7*

The distribution of the aneuploidy that was contributed by chromosome 1 and by chromosome 4 is detailed in the table as “Total % aneuploid cells”. The percent of cells with a gain in chromosome 1 and/or of chromosome 4 are indicated in the table under Gain. Cells with both chromosomes gained are indicated by “Change in both chromosomes”; ±standard deviation.

* $p < 0.05$.

Table 2

Percent of control and SWCNT-treated BEAS-2B cells in the different phases of the cell cycle.

	%G1	CV of G1	%S	%G2/M	CV of G2/M
PBS treated cells	40.15 ± 1.12	8.72 ± 0.47	35.49 ± 1.09	24.44 ± 0.87	8.27 ± 0.27
SWCNT-treated cells	43.10 ± 1.89	13.00 ± 1.54	28.99 ± 3.17	30.57 ± 2.56*	12.33 ± 1.55

CV: coefficient of variance; ±standard deviation.

* $p < 0.05$.